

Recent developments in background oriented schlieren methods for rotor blade tip vortex measurements

Kolja Kindler¹, Erik Goldhahn², Friedrich Leopold³, Markus Raffel⁴

1: Technical Flows, DLR Institute for Aerodynamics and Flow Technology, Göttingen, Germany,
kolja.kindler@dlr.de

2: Institute for Turbo Machinery, Technical University of Hannover, Hannover, Germany,
goldhahn@tfd.uni-hannover.de

3: Institute Franco-Allemand de Recherche de Saint-Luis (ISL), Saint-Luis, France, leopold@isl.tm.fr

4: Technical Flows, DLR Institute for Aerodynamics and Flow Technology, Göttingen, Germany,
markus.raffel@dlr.de

Abstract To date, the compressible blade tip vortex (BTV) in rotor flight has been subject of numerous investigations and its importance for the understanding of the helicopter flow field has clearly been drawn. Due to its great impact on the dynamics of the flow field, the investigation of the BTV is directly linked to issues of flow control and aeroacoustic optimisation. However, despite of the velocity field data of the BTV, additional density information for vortex modelling is desirable. In this work we present preliminary experimental results of background oriented schlieren (BOS) measurements on a 0.4 Mach scaled rotor model of the BO 105. This data is evaluated utilising a tomographic algorithm which enables us to compute an estimate of the vortex density field. This method is demonstrated to yield reasonable scales of the vortex core diameter. We discuss the advantages and applicability of the filtered back-projection (FBP) method on BOS images of the BTV. Furthermore, we report on first full-scale in-flight stereoscopic BOS measurements of the BTV on a BO 105 helicopter. Stereoscopic imaging utilising a non-correlating natural formation as the background allows for a reference free and therefore dynamic BTV detection.

Nomenclature

C_T	thrust coefficient	γ	deflection angle
c	blade chord length	δz	image distortion
$k_{x,y}$	spatial frequencies	$\delta\rho$	density variation
Ma	Mach number	ρ	density
n	index of refraction	Θ	projection angle
R	blade radius	σ	solidity
r_c	core radius		
x, y, z	cartesian coordinates		

1. Introduction

The tip vortex shed from revolving helicopter rotor blades is a compressible sharply localised vortical structure whose strength is known to scale with the blade tip Reynolds number McCroscey (1995), Leishman (1998). Depending on the flight attitude determining the relative distance and orientation of the vortex of a preparatory blade and the successive one blade-vortex interactions (BVI) might occur, which are considered a major source of aeroacoustic noise in rotor flight. Especially in low-speed descending flight or maneuvers the sound emission

as well as structural vibrations increase remarkably. Therefore, numerous experimental studies of the rotor flow field and the BVI have been conducted mostly employing Particle Image Velocimetry (PIV) (e.g. van der Wall and Richard (2005) and Richard et al (2006)). Beside the experimental approach, numerical simulation and corresponding aeroacoustic modeling of both the near and the far field are increasingly important tools in the investigation of helicopter aerodynamics Ehrenfried et al (1991), Strawn et al (1996). However, due to the complexity of the flow field, numerical investigations might be improved considerably by the support of experimental data on the density in the vortex core.

On the other hand, direct density measurements at the blade tip so far reported are mostly complicated and time consuming. Interferometric techniques for example rely on optical arrangements and lasers restricting those techniques to the laboratory use only (see for example Snyder and Hesselink (1984), Chandrasekhara et al (1995)). Therefore, it seems to be proximate to apply the Background Oriented Schlieren (BOS) technique with a view to BTV detection.

Commonly, the BOS technique is based on directly imaging a speckle pattern with and without an aerodynamic structure influencing the light path. The density gradients, introduced by a compressible and distinctively localised vortex for example, are related to gradients of the refractive index which are transferred into a deformation of the imaged background pattern. Hence, the vortex structure morphology can be reconstructed based on the an image-reference pair using robust and very efficient cross-correlation methods. For a detailed description of the BOS technique we refer to Meier (2002) and Raffel et al (2000).

Furthermore, implying a vortex such as the BTV to be rotational symmetric, the density field might be estimated based on BOS data using tomographic evaluation algorithms. As according to Richard et al (2006) the BTV sufficiently matches this symmetry condition¹, we use the filtered back-projection method applied to slices of two-dimensional BOS field data of hovering in ground effect in order to derive a density field estimate of the cross-section of the BTV. As the BOS data the evaluation is based on has to be regarded as preliminary, we do not attempt to quantitatively compare our results to the literature available but we emphasize the applicability of the evaluation scheme.

Extending this approach, we already conducted first full-scale tests on a BO 105 helicopter in flight. The basic idea was to setup a very simple hand-held sensor device which allows for dynamic reference free data acquisition associated with natural formations feasible as BOS backgrounds. According to Raffel et al (2000) non-correlating but homogeneous natural formations such as grass or leaves provide a sufficient background for the BOS technique. We used leaves of a skirt of wood in order to take advantage of their colour depth and large contrast. Furthermore, Gruppi et al (2005) introduced a procedure to apply weighted local colour separation thereby gaining an increase of the signal-to-noise ratio, which is also capable of artificially shrinking larger structures of the background. The main restriction for the in-flight imaging from within the fuselage with a view to BOS is the fairly short and fixed distance from the camera to the vortex. As the image shifting is expected to be rather weak, one cannot compensate for that by large image distances. Thus, the images of the stereoscopic system must be aligned very carefully as well as their resolution has to allow for comparatively small evaluation window sizes.

Briefly outlining the organisation of the article, we will depict the FBP algorithm in the next section and specify the experimental details of the work thereafter. Subsequently, we report the results of the tomographic evaluation and summarise the main conclusions.

¹The rotational symmetry of the BTV alludes to “young” vortices, in the close vicinity of the blade’s trailing edge.

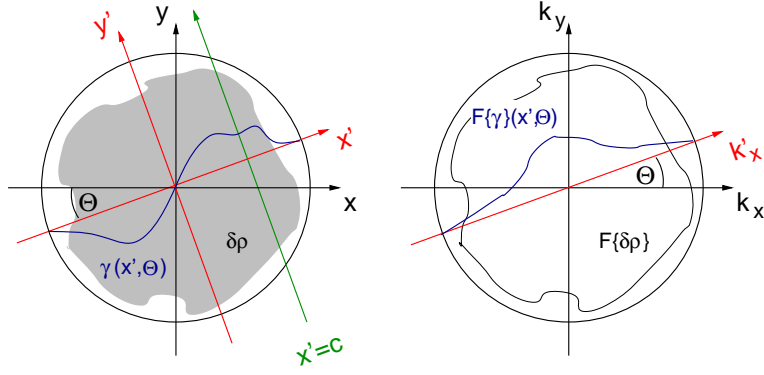


Figure 1: On the interpretation of the tomographic algorithm, a slice of a rotational symmetric density variation in physical (left) and Fourier space (right). The green line on the right represents the path of an example ray passing the density structure. See the text for further details.

2. Tomographic BOS data evaluation

Adopting the deflections of the light rays passing a density gradient to be sufficiently small the deflection angles $\gamma_{x,y}$ read:

$$\tan(\gamma_{x,z}) = \int \frac{\partial \rho}{\partial(x, z)} dy \quad . \quad (1)$$

The deflection might be regarded as the Radon transform (RT) of the density field with respect to the line of sight. The Radon transform itself is a well-known tool in medical tomographic imaging application and one might refer to Toft (1996) for a comprehensive review.

In Fig. 1 we sketch a slice of the density field of an idealised vortex. Introducing a coordinate system (x', y') wherein the line of sight is parallel to the y' -axis (see Fig. 1 on the left), the Radon transform of the density along the line of sight takes the form:

$$\begin{aligned} R\{\rho\}(x', \Theta) &= \int_{-\infty}^{\infty} \rho(x, y) dt \\ &= \int_{-\infty}^{\infty} \rho(x' \cdot \cos(\Theta) - y' \cdot \sin(\Theta), y' \cdot \cos(\Theta) + x' \cdot \sin(\Theta)) dy' \end{aligned} \quad (2)$$

and the corresponding Fourier transform of $R\{\rho\}$

$$\begin{aligned} F\{R\{\rho\}\}(k'_x, \Theta) &= \int_{-\infty}^{\infty} \int_{-\infty}^{\infty} \rho(x' \cdot \cos(\Theta) - y' \cdot \sin(\Theta), \dots \\ &\quad y' \cdot \cos(\Theta) + x' \cdot \sin(\Theta)) \cdot e^{-i \cdot 2\pi \cdot k'_x \cdot x'} dy' dx' \\ &\equiv \aleph(k'_x, \Theta) \quad , \end{aligned} \quad (3)$$

which is sketched in Fig. 1 also.

The Fourier transform of the deflection angles

$$\begin{aligned}
F\{\gamma\}(k'_x, \Theta) &= \int_{-\infty}^{\infty} \gamma(x', \Theta) \cdot e^{-i \cdot 2\pi \cdot k'_x \cdot x'} dx' \\
&= D \int_{-\infty}^{\infty} \int_{-\infty}^{\infty} \frac{\partial \rho}{\partial x'} \cdot e^{-i \cdot 2\pi \cdot k'_x \cdot x'} dy' dx' \\
&= D \cdot i \cdot 2\pi \cdot k'_x \cdot \aleph(k'_x, \Theta) \\
&\equiv \Gamma(k'_x, \Theta)
\end{aligned} \tag{4}$$

with D being some constant, leads to the relation of the deflection angles and the RT of the density. Inverting the Fourier transform of $R\{\rho\}$ using polar coordinates one writes

$$\begin{aligned}
\rho(x, y) &= \rho(x' \cdot \cos(\Theta) - y' \cdot \sin(\Theta), y' \cdot \cos(\Theta) + x' \cdot \sin(\Theta)) \\
&= \int_0^{2\pi} \int_0^{\infty} \aleph(k'_x, \Theta) \cdot e^{i \cdot 2\pi \cdot k'_x \cdot x'} dy' dx' \\
\rho(x, y) &= \int_0^{\pi} \int_{-\infty}^{\infty} \aleph(k'_x, \Theta) \cdot |k'_x| \cdot e^{i \cdot 2\pi \cdot k'_x \cdot x'} dy' dx' \\
&= \int_0^{\pi} \int_{-\infty}^{\infty} \underbrace{\frac{|k'_x|}{D \cdot i \cdot 2\pi \cdot k'_x}}_{\equiv Q(k'_x)} \cdot \Gamma(k'_x, \Theta) \cdot e^{i \cdot 2\pi \cdot k'_x \cdot x'} dy' dx'
\end{aligned} \tag{5}$$

wherein Q is a filter applied to Γ in Fourier space. Equation 5 basically resembles the Fourier slice theorem.

Taking into account the convolution theorem Eqn. 5 is equivalent to:

$$\rho(x, y) = \int_0^{\pi} q(x') * \gamma(x', \Theta) d\Theta \tag{6}$$

with

$$q(x') = F^{-1}\{Q(k'_x, \Theta)\} \quad \text{and} \quad \gamma(x', \Theta) = F^{-1}\{\Gamma(k'_x, \Theta)\} \quad .$$

Henceforth, we are able to specify the density field based on the image deflections measured and the known distance of the vortex. Filtering the deflection angles with $Q(k'_x)$ in Fourier space and computing the inverse transformation yields the density field data.

3. Experimentals

The experimental setup in the rotor testing hall of DLR Braunschweig is the same as described by Richard et al (2006). A 40% dynamically Mach-scaled model of the MBB BO-105 main rotor was used ($R=2$ m and $c=20.121$ m chord length). The blades possess a 2.5° pre-cone at the hub and a rectangular plan form featuring $-8^\circ/R$ linear twist at a solidity of $\sigma=0.077$. The BOS results to be presented refer to the rotor operating in ground effect at tip Mach numbers

of $Ma=0.633$ and at thrust coefficients of $C_T=0.0028$.

The BOS setup consisted of a PCO SensiCam in connection with a 300 mm lense observing a homogeneously illuminated speckle pattern from above the rotor plane. The camera was positioned at a distance of $3.289R$ with respect to the measurement volume with the background being another $5.289R$ away. The extension of the imaging plane is $1024 \times 1280 \text{ px}^2$ with a resolution of approximately 7.34 px/mm Subsequently, the raw data was processed using the PivView software by PivTech.

The stereoscopic BOS for in-flight testing systems consisted of two high resolution Canon OES 1D Mark II cameras with a 70 to 200 mm zoom objective mounted on an X95 profile, aligned vertically and placed behind the co-pilot’s seat. The sensor unit remained flexible during the test in order to manually aim at the blade tip position. The BO 105 has a main rotoor radius of $R = 4.98 \text{ m}$ and a chord length of $R = 0.2 \text{ m}$. The images were recorded at approximately 2 px/mm and 11 px/mm resolution with the 70 mm and 70 mm objective respectively. The cameras were parallelised and the spacing in between optimised to gain an image separation of $0.5c$ in the blade tip plane. The BO 105 The distance between the camera and the expected tip vortex position is approximately R while the distance to the background varied between 20–100 m. The measurements were conducted in very low-level hover flight at an altitude less than R .

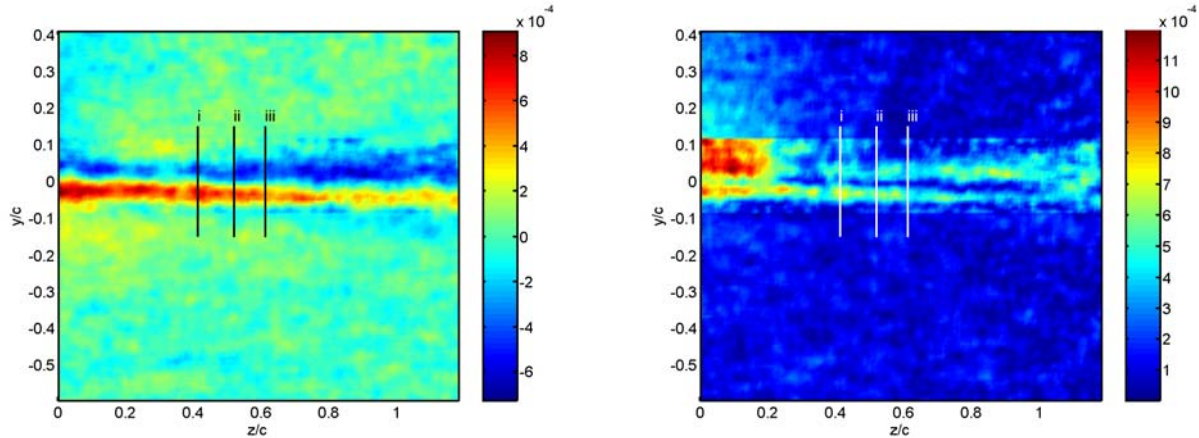


Figure 2: Image displacement (mm) of the y -component (left) and the in-plane magnitude of displacement (mm) (right) of the BTV at $Ma=0.633$ and $C_T=0.0049$.

4. Results

Figure 2 shows an example of a BOS result of the BTV in the vicinity of the blade. The main deflections are observed in the y -component, while the chordwise x -component turns out to be fairly noisy. However, the vortex is fully developed at the trailing edge and starts to spread increasing its core radius at approximately $z \simeq 0.5c$ We note that due to limitations of the light intensity mainly determining the exposure time, the BOS data is biased by smear effects of the blade. The area of cohesive positive in-plane deflection magnitude closely above the blade tip is probably an artefact of smearing ((0, -0.1) in Fig. 2 corresponds to the position of the trailing edge of the blade tip). Therefore, the instantaneous BOS results imply a spatial average of approximately 5° and additionally a conditional average is calculated from series of ten images in order to enhance the signal. These averaged fields are evaluated by means of filtered back-

projection at three different chordwise positions. Considering these averaging effects smearing the narrow vortex core, we expect the density to be underestimated by the FBP in addition to effects of the rather poor spatial resolution.

Figure 3 depicts the deflection data analysed (sliced at the positions i,ii and iii in Fig. 2) and the corresponding density estimates. The three slices are extracted from the field data at $0.41c$, $0.52c$ and $0.61c$ downstream the trailing edge of the blade. The vortex structure can

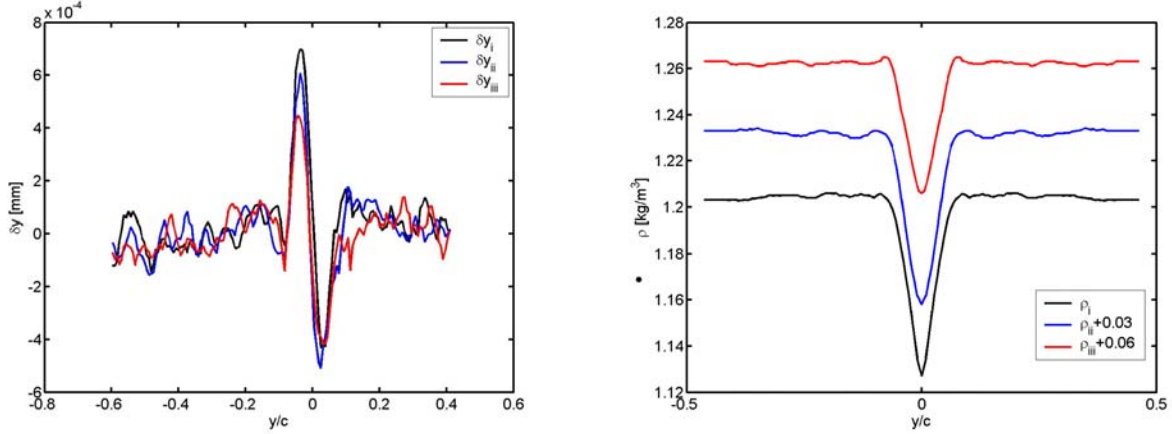


Figure 3: Image displacement of the y -component (left) and the corresponding density estimates (right) at the three positions given in Fig. 2. The density is azimuthally averaged with respect to the vortex core position in the y - z -plane.

clearly be identified, although the deflections are not symmetric at all three positions. We mainly attribute this lack of symmetry to the measurements uncertainties.

Application of FBP implying standart atmospheric conditions and $T = 20^\circ\text{C}$ yields the density shown on the right of Fig. 3 exhibiting central core density drops of the order of 10% slightly decreasing with increasing distance from the trailing edge and the onset of lateral swelling. The limited density drop can be identified with the effects of smearing already quoted above. It is commonly accepted that a vortex core diameter according to $r_c \simeq 0.05 \cdot c$ can be expected based on velocity van der Wall and Richard (2005). The density distribution we estimate has an extension of approximately $0.20c$ which is slightly larger than the velocity based value of the core given above.

With a view to the in-flight test first of all we note that the light intensity essential to acquire BOS data of adequate resolution turns out to be a severe issue. Although the measurements profited from sunny and cloudless conditions, we had to reduce to the 70 mm-lense in order to suppress smearing of the blade.

The low resolution of the 70 mm-lense images strongly hampers the data evaluation, because of the very narrow evaluation windows necessary to unambiguously identify the vortex.

However, we realised that the leave density and remainders of tree trunks demands further post-processing of the images.

5. Conclusions

The tip vortex in the vicinity of the rotor blade has been visualised by means of the Background Oriented Schlieren technique on a 40% Mach-scaled rotor model of the BO 105. the results have been quantified by estimating the density of the core region utilising the filtered back

projection method. The vortex core diameter returned is on reasonable scales while the extent of the density drop within the vortex core remains under-estimated. However, we demonstrated the evaluation of planar BOS data with the aid of a tomographic algorithm to be successfully applicable to young blade tip vortices.

Furthermore, the full-scale in-flight measurements with the BO-105 test-helicopter in hover flight are reported. Utilising a hand-held stereoscopic BOS system we recorded the blade tips with various magnifications from the fuselage. We note...

Unfortunately, we cannot give any results of the full-scale testing yet because the data processing is not finished by the time of the submission deadline, but we look forward to show first results during the conference. Although, the full-scale application is hampered by various difficulties and limitations, in-flight measurements and subsequent core density estimations are a promising task aiming at an improved understanding of the flow field dynamics.

References

- Chandrasekhara M, Squires D, Wilder M, Carr L (1995) A phase-locked high-speed real-time interferometry system for large amplitude unsteady flows. *Exp Fluids* 20(2):61
- Ehrenfried K, Meier G, Obermeier F (1991) Sound produced by vortex-airfoil interaction. In: 17th ERF, Berlin, Germany
- Gruppi D, Guernier S, Leopold F, Schäfer H (2005) Mehrfarben-Hintergrund-schlieren-Technik (CBOS) zur Vermessung der Lichtablenkung von Dichtegradienten. In: Fachtagung Lasermethoden in der Strömungsmechanik, Sep. 6-8th 2005, BTU Cottbus (in german)
- Leishman J (1998) Measurement of the aperiodic wake of a hovering rotor. *Exp Fluids* 25:352
- McCroscey W (1995) Vortex wake of rotor craft. In: 33th AIAA Aerospace Science Meeting and Exhibit, Reno, USA
- Meier G (2002) Computerized background-oriented schlieren. *Exp Fluids* 3:181
- Raffel M, Tung C, Richard H, Yu Y, Meier G (2000) Background oriented stereoscopic schlieren (boss) for full scale helicopter vortex characterization. In: 9th Int. Symp. on Flow Visualization, Heriot-Watt University, Edinburgh, G.B.
- Richard H, Bosbach J, Henning A, Raffel M, van der Wall B (2006) 2c and 3c piv measurements on a rotor in hover condition. In: 13th Int. Symp. on Applications of Laser Techniques to Fluid Mechanics, 26-29th June, Lisbon, Portugal
- Snyder R, Hesselink L (1984) Optical tomography for flow visualization of the density field around a revolving helicopter blade. *Appl Optics* 23(20):3650
- Strawn R, Olikier L, Biswas R (1996) New computational methods for the prediction and analysis of helicopter noise. In: 2nd AIAA/CEAS Aeroacoustic Conference, May 1996, State College, PA, USA
- Toft P (1996) The radon transform, theory and implementation. Ph.D. thesis, Technical University of Denmark, Kogens Lyngby, Denmark
- van der Wall B, Richard H (2005) Visualization of vortical structures by density gradient detection. In: The 2nd Int. Basic Research Conference on Rotorcraft Technology, Nov 7-9th, Nanjing, China